Trapping of single atoms in cavity QED

J. Ye, D. W. Vernooy, and H.J. Kimble

Norman Bridge Laboratory of Physics, California
Institute of Technology 12-33, Pasadena, CA 91125

(October 19, 2018)

By integrating the techniques of laser cooling and trapping with those of cavity quantum electro-dynamics (QED), single Cesium atoms have been trapped within the mode of a small, high finesse optical cavity in a regime of strong coupling. The observed lifetime for individual atoms trapped within the cavity mode is $\tau \approx 28$ms, and is limited by fluctuations of light forces arising from the far-detuned intracavity field. This initial realization of trapped atoms in cavity QED should enable diverse protocols in quantum information science.

Cavity quantum electrodynamics (QED) offers powerful possibilities for the deterministic control of atom-photon interactions quantum by quantum. [1,2] Indeed, modern experiments in cavity QED have achieved the exceptional circumstance of strong coupling, for which single quanta can profoundly impact the dynamics of the atom-cavity system. Cavity QED has led to many new phenomena, including the realization of a quantum phase gate, [3] the creation of Fock states of the radiation field, [4] and the demonstration of quantum nondemolition detection for single photons [5].

These and other diverse accomplishments set the stage for advances into yet broader frontiers in quantum information science for which cavity QED offers unique advantages. For example, it should be possible to realize complex quantum circuits and quantum networks by way of multiple atom-cavity systems linked by optical interconnects, [6,7] as well as to pursue more general investigations of quantum dynamics for continuously observed open quantum systems [8]. The primary technical challenge on the road toward these scientific goals is the need to trap and localize atoms within a cavity in a setting suitable for strong coupling. In fact, all proposed schemes for quantum computation and communication via cavity QED rely implicitly on the development of techniques for atom confinement that do not interfere with cavity QED interactions.

In this Letter we report a significant milestone in this quest, namely the first trapping of a single atom in cavity QED. Our experiment integrates the techniques of laser cooling and trapping with those of cavity QED to deliver cold atoms (kinetic energy $E_k \simeq 30\mu$K) into the mode of a high finesse optical cavity. In a domain of strong coupling, the trajectory of an individual atom within the cavity mode can be monitored in *real time* by a near resonant field with mean intracavity photon number $\bar{n} < 1$ [9–13]. Here we exploit this capability to trigger *ON* an auxiliary field that functions as a far-off resonance dipole-force trap (FORT) [14,15], providing a confining potential to trap the atom within the cavity mode. Likewise, when the FORT is turned *OFF* after a variable delay, strong coupling enables detection of the atom. Repetition of such measurements yield a trap lifetime $\tau = (28 \pm 6)$ms,

which is currently limited by fluctuations in the intensity of the intracavity trapping field (FORT).

Stated in units of the coupling parameter g_0 (where $2g_0$ is the single-photon Rabi frequency), our work achieves $g_0\tau \simeq 10^6\pi$, whereas prior experiments with cold atoms have attained $g_0T \simeq 10^4\pi$ [9–13] and experiments with conventional atomic beams have $g_0T \simeq \pi$, [1–5] with T as the atomic transit time through the cavity mode. Finally, as a step toward *in situ* monitoring of an atom within the FORT we describe observations of the transmission of a cavity QED probe field in the presence of the trapping potential for single atom transits.

Our experimental apparatus consists of a high finesse cavity, two-stage magneto-optical traps (MOT), and cavity probe, lock, and FORT beams, as shown in Figure 1. Roughly 10^8 Cesium atoms are accumulated in an "upstairs" MOT-1, cooled with polarization gradients to 3μK, and then transferred with 10% efficiency to a "downstairs" MOT-2 located in a UHV chamber with background pressure 10^{-10}Torr. The captured atoms are next cooled to 2μK and dropped from a position 5mm above a high finesse optical cavity. Some few atoms fall between the cavity mirrors, and thence through the cavity mode itself.

A final stage in the protocol for delivering cold atoms into the mode volume is provided by a set of cooling beams located in the $y - z$ plane perpendicular to the cavity axis, as shown in Fig. 1 (b). These beams form two independent standing waves along the $\pm 45°$ directions in the $y - z$ plane, each with helical polarization, and are switched on for 1.5ms to remove the residual fall velocity of atoms arriving at the cavity mode from MOT-2, leading to final velocities $v \sim 5$cm/s for atoms in the immediate vicinity of the cavity mode.

The Fabry-Perot cavity into which the atoms fall is formed from two super-polished spherical mirrors. The cavity length $l = 44.6\mu$m, waist $w_0 = 20\mu$m, and finesse $\mathcal{F} = 4.2 \times 10^5$, and hence a cavity field decay rate $\kappa/2\pi = 4$MHz [16]. The atomic transition employed for cavity QED is the ($g \equiv 6S_{1/2}, F = 4, m_F = 4 \to e \equiv 6P_{3/2}, F = 5, m_F = 5$) component of the D_2 line of atomic Cesium at $\lambda_{atom} \equiv c/\nu_{atom} = 852.4$nm. For our cavity geometry and from the atomic transi-

tion properties, we have $(g_0, \gamma_\perp)/2\pi = (32, 2.6)$MHz, with g_0 as the peak atom-field coupling coefficient and $\gamma_\perp$ as the dipole decay rate for the $e \to g$ transition. These rates lead to critical photon and atom numbers $(m_0 \equiv \gamma_\perp^2/2g_0^2, N_0 \equiv 2\kappa\gamma_\perp/g_0^2) = (0.003, 0.02)$.

The cavity length is stabilized with an auxiliary diode laser $\lambda_{lock} \equiv c/\nu_{lock} \approx 836$nm, which is stabilized relative to ν_{atom} by way of an auxiliary "transfer cavity" [11]. It is detuned 2 longitudinal-mode orders *above* the cavity QED mode at $\nu_{cavity} \approx \nu_{atom}$, and creates a small AC Stark shift of 50kHz in ν_{atom}. Residual fluctuations in the length of the locked cavity lead to variations in $\Delta_{ac} \equiv \nu_{atom} - \nu_{cavity}$ of $\delta\Delta_{ac} \approx \pm 10$kHz contained within a locking bandwidth of about 10kHz.

The "trajectory" of an individual atom is monitored in real time as it enters and moves within the cavity mode by recording modifications of the (pW-scale) cavity transmission for a circularly polarized probe field $\mathcal{E}_{probe}$ of frequency $\nu_{probe} = \nu_{atom} + \Delta_{probe}$. For our Fabry-Perot cavity, the spatially dependent coupling coefficient $g(\vec{r}) = g_0 \sin(2\pi x/\lambda_{cavity}) \exp(-(y^2+z^2)/w_0^2) \equiv g_0\psi(\vec{r}, \lambda_{cavity})$, with the mirrors located at $x = (0, l)$. Heterodyne detection of the transmitted probe (with overall efficiency 47%) allows inference of the atomic position in a fashion that can be close to the standard quantum limit [11].

For the purpose of atomic trapping, the transmitted probe beam can be employed to trigger *ON* a far-off-resonance trap (FORT) [14,15] given the detection of an atom entering the mode volume. Here, the FORT beam is derived from an external diode laser locked to a cavity mode at $\lambda_{FORT} = c/\nu_{FORT} = 869$nm, two longitudinal-mode orders *below* the cavity QED mode at ν_{cavity}. In this case, the standing-wave patterns of the two modes at $(\nu_{FORT}, \nu_{cavity})$ are such that there are approximately coincident antinodes near the center and ends of the cavity; hence, the trapping potential of the FORT has maximum depths at the positions of maxima (g_0) for cavity QED coupling in these regions.

An example of the trapping of a single atom is given in Figure 2. In (a) the arrival of an atom is sensed by a reduction in transmission for the probe beam (of photon number $\bar{n} \approx 0.1$ [17]). The falling edge of the probe transmission triggers *ON* the FORT field, which then remains on until being switched *OFF* after a fixed interval. The presence of the atom at this *OFF* time is likewise detected by modification of the probe transmission, demonstrating a trapping time of 13.5ms for the particular event shown in the figure. Note that because the probabilities for atom trapping given a trigger $p_{tp|tg}$ and for detection given a trapped atom $p_{d|tp}$ are rather small ($p_{tp|tg}p_{d|tp} \sim 0.03$), we operate at rather high densities of cold atoms, such that the average atom number present in the cavity mode at the time of the trigger is $\bar{N}_{atom} \sim 0.5$ (but which then falls off rapidly). As a consequence, the atom that causes the trigger is not always the atom that is actually trapped when the FORT

is gated *ON*, with such 'phantom' events estimated to occur in roughly 1 of 4 cases.

The timing diagram for switching of the various fields is given in Figure 2(b). Note that although the probe field is left on for all times in Fig. 2(a), there is no apparent change in cavity transmission during the interval in which an atom is purportedly trapped within the cavity mode. The absence of atomic signatures during the trapping time, but not before or after, is due to AC-Stark shifts associated with the FORT and/or the mismatched antinodes between $(\nu_{FORT}, \nu_{cavity})$. For the data of Figure 2, a power of 30μW incident upon the cavity at λ_{FORT} leads to a circulating intracavity power of 1W, and to AC-Stark shifts $\Delta_{FORT}^{e,g} = \pm 45$MHz for the excited e and ground g states at the cavity antinodes, so that at these locations, the net atomic transition frequency ν_{atom} is shifted to the blue by $\Delta_{FORT}^e - \Delta_{FORT}^g \equiv \Delta_{FORT} = +90$MHz. Moreover, the spatial dependence of the cavity mode means that $\Delta_{FORT}^{e,g}(\vec{r}) = \Delta_{FORT}^{e,g}\psi(\vec{r}, \lambda_{FORT})$, so that the FORT effectively provides a spatially dependent detuning that shifts the cavity QED interactions out of resonance, with $\Delta_{ac} \to \Delta_{ac} + \Delta_{FORT}(\vec{r})$. To calculate the probe transmission in this case requires an analysis of the eigenvalue structure incorporating both the coupling $g_0(\vec{r})$ as well as $\Delta_{FORT}(\vec{r})$ [18].

To avoid questions related to the complexity of this eigenvalue structure as well as to possible heating or cooling by the probe field, we synchronously gate *OFF* the probe field $\mathcal{E}_{probe}$ for measurements of trap lifetime, with the result displayed in Figure 3. These data are acquired for repeated trials as in Fig. 2 (namely, with the presence of an atom used to trigger *ON* the FORT now of depth $\Delta_{FORT}^g = -50$MHz), but now with the probe field gated *OFF* after receipt of a valid trigger (as shown by the solid trace for $\mathcal{E}_{probe}$ in Fig. 2(b)). At the end of the trapping interval, $\mathcal{E}_{probe}$ is gated back *ON*, and the success (or failure) of atomic detection recorded. The lifetime for single atoms trapped within the FORT is thereby determined to be $\tau_{FORT} = (28 \pm 6)$ms. This trap lifetime is confirmed in an independent experiment where the FORT is turned on and off at predetermined times without transit-triggering, yielding $\tau'_{FORT} = (27 \pm 6)$ms. As mentioned in the discussion of Fig. 2, our ability to load the trap with reasonable efficiency via asynchronous turn-on is due to operation with large $\bar{N}_{atom}$.

Note that at each of the time delays in Fig. 3, a subtraction of "background" events (atomic transits delayed by the intracavity cooling beams) has been made from the set of total detected events. We determine this background by way of measurements following the same protocol as in Fig. 2(b), but without the FORT beam. For times below 10ms in Fig. 3, this background dominates the signal by roughly 50-fold, precluding accurate measurements of trapped events. However, because it has a rapid decay time ≈ 3ms, for times greater than about 20ms it makes a negligible contribution.

2

As for the factors that limit the trap lifetime, the spontaneous photon scattering rate is 37 s^{-1} in our FORT. The trap lifetime set by background gas collisions at a pressure of 10^{-10} Torr is estimated to be ~ 100s, which is likewise much longer than that actually observed. However, Savard et al. [19] have shown that laser intensity noise causes heating in a FORT with heating rate $\tau_e^{-1} = \pi^2 \nu_{tr}^2 S_e(2\nu_{tr})$ (Eq. (12) of Ref. [19]). Here ν_{tr} is the trap oscillation frequency (in cycles/s) and $S_e(2\nu_{tr})$ is power spectral density of fractional intensity noise evaluated at frequency $2\nu_{tr}$. For the FORT of Figure 3, we estimate $(\nu_{tr}^{radial}, \nu_{tr}^{axial}) \approx (5, 450)$kHz for the radial (y, z) and axial x directions, respectively. Direct measurements of the spectral density of photocurrent fluctuations for the FORT beam emerging from the cavity (calibrated by coherent AM at the requisite frequency $2\nu_{tr}$) lead to $(S_e(2\nu_{tr}^{radial}), S_e(2\nu_{tr}^{axial})) \approx (5 \times 10^{-9}, 2.3 \times 10^{-11})$/Hz, so that $(\tau_e^{radial}, \tau_e^{axial}) \approx (830, 23)$ms. The heating rate for $1/\tau_e^{axial}$ is in reasonable agreement with the observed $(1/e)$ trap decay rate $1/\tau_{FORT} \simeq 1/28$ms, leading to the conclusion that fluctuations in intracavity intensity drive heating along the cavity axis and are the limiting factor in our current work. Such fluctuations are exacerbated by the conversion of FM to AM noise of the FORT laser due to the high cavity finesse at the wavelength of the FORT (here, $\mathcal{F}_{FORT} = 3.5 \times 10^5$). An avenue to reduce $S_e(2\nu_{tr}^{axial})$ is by way of active servo control of the intensity of the intracavity FORT field (in addition to a wider bandwidth frequency servo that keeps the FORT field locked to the cavity resonance), which is a strategy that we are pursuing.

Finally, we return to the more general question of cavity QED in the presence of the FORT. As a starting point in a more complete investigation, Figure 4 displays a series of four atomic transits, each of increasing duration. With the FORT *OFF*, the "down-going" transit in (a) arises from an atom that was dropped from MOT-2 without the application of the cooling pulse shown in Fig. 2(b) and provides a reference for the time of free fall through $\psi(\vec{r}, \lambda_{cavity})$ (here, $T \approx 100\mu$s for $v \approx 30$cm/s). By contrast, with the cooling pulse applied (but with the FORT still *OFF*), the transit in (b) is lengthened to $T \approx 420\mu$s. In (c), Δ_{probe} is altered to sense "up-going" transits, with now $T \approx 1$ms. Because the kinetic energy of an atom with $v \sim 5$cm/s is much smaller than the coherent coupling energy $\hbar g_0$, it is possible to achieve long localization times via the single-photon trapping and cooling mechanisms discussed in Refs. [20,21], which can be understood by way of a simple 'Sisyphus'-picture based upon the spatially dependent level structure in cavity QED. For the last trace in (d), the FORT is always *ON* (i.e., not gated as in Fig. 2), but with a shallower potential ($\Delta_{FORT}^g = -15$MHz) than that in Fig. 2(a). We select the detunings $\Delta_{probe} = -10$MHz and $\Delta_{ac} = -10$MHz to enhance observation of a trapped atom via the composite eigenvalue structure associated with $g(\vec{r})$ and $\Delta_{FORT}(\vec{r})$ [22]. We also expect that cavity-assisted Sisyphus cooling [21] should be effective in this setting. As in (d), this results in remarkable 'transits' observed in real-time with $T \approx 7$ms, corresponding to transit velocity $\bar{v} \equiv \frac{2w_0}{T} \approx 6$mm/s and associated kinetic energy $\frac{1}{2}m\bar{v}^2 \sim h\nu_{tr}^{radial} \ll h\nu_{tr}^{axial}$.

In conclusion, although these are encouraging first results for trapping of single atoms in cavity QED, an outstanding problem with dipole-force traps is that the excited state experiences a positive AC Stark shift, leading to an excited state atom being *repelled* from the trap (e.g., during quantum logic operations). As well, the effective detuning $\Delta_{ac}(\vec{r}) \equiv \Delta_{ac} + \Delta_{FORT}(\vec{r})$ is a strong function of the atom's position within the trap. Fortunately, it turns out that a judicious choice of λ_{FORT} can eliminate both of these problems by making $\Delta_{FORT}^e(\vec{r}) = \Delta_{FORT}^g(\vec{r}) < 0$, and hence $\Delta_{FORT}(\vec{r}) = 0$ [23]. Alternatively, even for the current setup, it should be possible to tune Δ_{FORT}^e together with Δ_{ac} to produce regions within the cavity mode for which the spatially dependent level shift of a composite dressed state in the first excited manifold matches $\Delta_{FORT}^g(\vec{r})$ for the (trapping) ground state [22], as was attempted in Fig. 4 (d). These schemes in concert with extensions of the capabilities presented in this Letter should allow us to achieve atomic confinement in the Lamb-Dicke regime (i.e., $\eta_x \equiv 2\pi\Delta x/\lambda \ll 1$) in a setting for which the trapping potential for the atomic center-of-mass motion is independent of internal atomic state, as has been so powerfully exploited with trapped ions [24]. Generally speaking, this essential task must be completed for long-term progress in quantum information science via photon-atom interactions.

[1] *Cavity Quantum Electrodynamics,* ed. P. Berman (Academic Press, San Diego, 1994).
[2] For a more recent review, see contributions in the Special Issue of Physica Scripta **T76** (1998).
[3] Q. A. Turchette et al., Phys. Rev. Lett. **75**, 4710(1995).
[4] Walther et al., *Fourteenth International Conference on Laser Spectroscopy*, Innsbruck, June, 1999.
[5] G. Nogues et al., Nature **400**, 239 (1999).
[6] T. Pellizzari, et al., Phys. Rev. Lett. **75**, 3788 (1995).
[7] J.-I. Cirac, et al., Physica Scripta **T76**, 223 (1998).
[8] H. Mabuchi and H. Wiseman, Phys. Rev. Lett. **82**, 1798 (1999).
[9] H. Mabuchi, Q. A. Turchette, M. S. Chapman, and H. J.

Kimble, Opt. Lett. **21**, 1393 (1996).

[10] C. J. Hood, M. S. Chapman, T. W. Lynn, and H. J. Kimble, Phys. Rev. Lett. **80**, 4157 (1998).

[11] H. Mabuchi, J. Ye, and H. J. Kimble, Appl. Phys. B**68**, 1095 (1999).

[12] J. Ye et al., IEEE Trans. Instru. & Meas. **48**, 608 (1999).

[13] P. Müstermann et al., Phys. Rev. Lett. **82**, 3791 (1999).

[14] J. D. Miller, R. A. Cline, and D. J. Heinzen, Phys. Rev. **A47**, R4567 (1993).

[15] H. J. Lee, C. S. Adams, M. Kasevich, and S. Chu, Phys. Rev. Lett. **76**, 2658 (1996).

[16] The differential phase shift between the cavity eigen-polarizations is $\Delta\beta = 2\mu$rad/bounce.

[17] Throughout, $\bar{n}$ specifies the mean intracavity photon number for the empty cavity (i.e., no atoms) at the actual detuning Δ_{probe}.

[18] D. W. Vernooy and H. J. Kimble, Phys. Rev. **A56**, 4287 (1997).

[19] T. A. Savard, K. M. O'Hara, and J. E. Thomas, Phys. Rev. **A56**, R1095 (1997).

[20] A. C. Doherty et al., Phys. Rev. **A56**, 833 (1997).

[21] P. Horak, et al., Phys. Rev. Lett. **79**, 4974 (1997).

[22] J. Ye, D. W. Vernooy, and H. J. Kimble, in preparation (1999).

[23] C. J. Hood and C. Wood, in preparation (1999).

[24] D. Leibfried et al., Phys. Rev. Lett. **77**, 4281 (1996).

FIG. 2. (a) A single atom (curve (i), with 30 kHz bandwidth) is detected within the cavity mode and triggers *ON* a dipole-force trap (FORT, curve (ii)). When the FORT is switched *OFF* after a 13.5 ms delay, the atom is detected again. $\Delta_{probe} = 0 = \Delta_{ac}$, $\Delta^g_{FORT} = -45$MHz, and $\bar{n} = 0.1$photons. (b) Timing sequence for the release of MOT-2, intra-cavity cooling, single atom detection, and loading of the FORT. The polarization-gradient cooled atoms are released at time t_0 (0 ms). Under the condition of no cooling pulse and no FORT, atoms reach the cavity mode between 27 to 37 ms. The cooling pulse is switched *ON* and the FORT switched *OFF* at t_1 (34 ms). The cooling beams are then detuned further by 18MHz and their intensities decreased between t_2 (35 ms) and t_3 (35.5 ms). At the end of cooling (t_3) the cavity probe is turned *ON*. Once a single atom is detected, for example at t_4, which varies within a 3 ms window, the FORT is switched *ON* and the cavity probe *OFF*. After a predetermined delay, ($t_5 - t_4$), the FORT is turned *OFF* and the cavity probe *ON* for detection (t_5). At t_6 everything is reset for the next cycle. For the data shown in curve (a) (i), the cavity probe was left on continuously (dashed line in (b)).
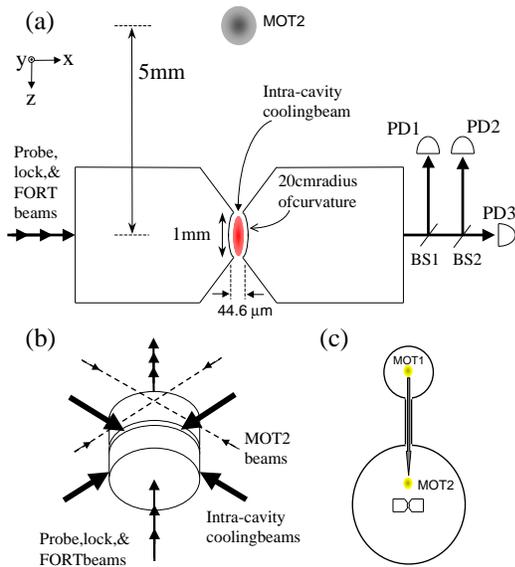

FIG. 1. Schematic of the experimental apparatus. (a) The dichroic beam splitter BS1 sends the cavity-length-stabilizing beam to PD1. BS2 separates the FORT (sent to PD2 for locking) and cavity QED beams (sent to PD3 for balanced heterodyne detection). (b) Beam geometry for intra-cavity cooling and MOT-2. (c) Differentially pumped chamber and the two-stage MOT.
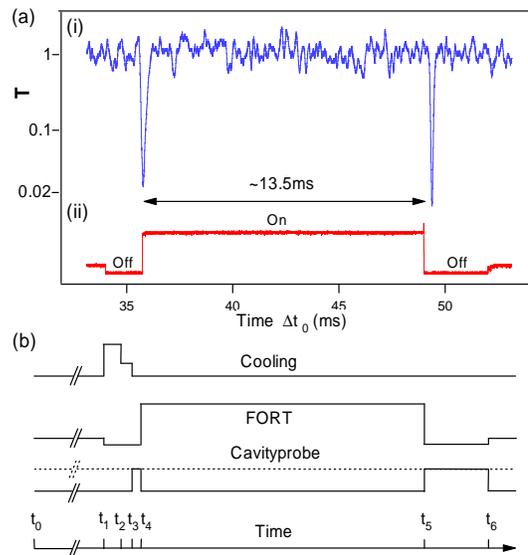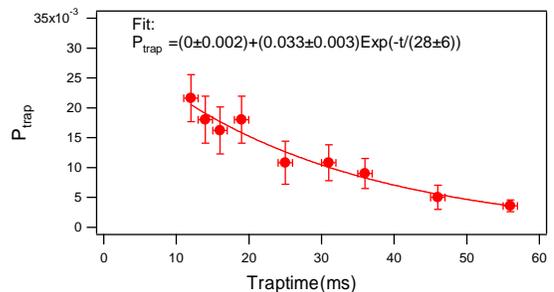

FIG. 3. Measurement of trap lifetime τ_{FORT} (see text). For these data, the FORT is triggered *ON* by single atom transits in the time window (t_3, t_4) of Fig. 2(b). P_{trap} gives the probability per trigger of successful detection of a trapped atom in the time window (t_5, t_6). The exponential fit results in $\tau_{FORT} = 28 \pm 6$ms.
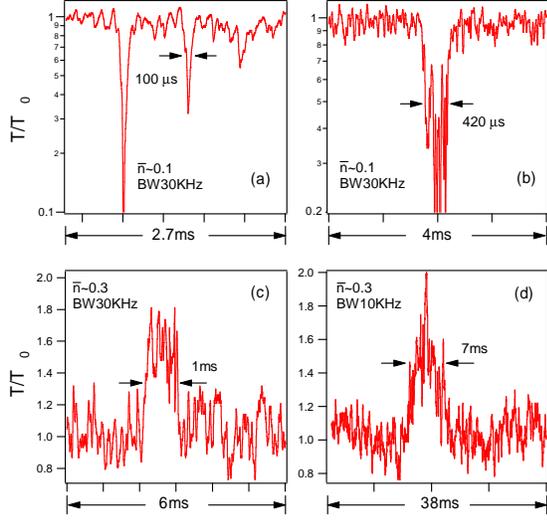
FIG. 4. Representative transits under four different conditions. (a) Atom free falls, $\Delta_{probe} = 0 = \Delta_{ac}$. (b) Intra-cavity cooling *ON*, $\Delta_{probe} = 0 = \Delta_{ac}$ (c) Intra-cavity cooling *ON*, $\Delta_{probe} = -30$MHz, $\Delta_{ac} = 0$. (d) Both intra-cavity cooling and FORT *ON*, $\Delta_{probe} = -10$MHz, $\Delta_{ac} = -10$MHz, and $\Delta_{FORT}^{g} = -15$MHz.